Cross Section Measurement at High Q^2

B. Reisert [a]

[a]Max-Planck-Institut für Physik, Föhringer Ring 6, D-80805 München, reisert@mppmu.mpg.de

The inclusive single and double differential cross sections for neutral and charged current processes with four-momentum transfer squared Q^2 between 150 and 30000 GeV^2 are measured with the H1 detectors at HERA. Data on e^+p interactions have been collected from 1994-97 and correspond to an integrated luminosity of about 36 pb^{-1}. Preliminary e^-p results are based on data collected in 1998 and beginning of 1999 with an integrated luminosity of 5.6 pb^{-1}. Predictions of the electroweak theory are confronted with the data. No significant deviation from the Standard Model has been found. The consistency of the theoretical expectation with the data is expressed by the measured mass of the W boson and by the observed difference in e^-p and e^+p neutral current cross-sections at high Q^2 due to γZ interference.

1. INTRODUCTION

1.1. Kinematic

In deep inelastic scattering (DIS) at high Q^2 the proton is probed at very short distances $< 10^{-18}m$. The kinematics of the DIS process is defined by three variables: the boson virtuality Q^2, the Bjorken scaling variable x, i. e. the proton momentum fraction carried by the struck quark, and the inelasticity y. At fixed center of mass energy $\sqrt{s}$ two variables are independent, y can be expressed by $y = Q^2/xs$.

From 1994-97 HERA was running with positrons of 27.5 GeV colliding on protons of 820 GeV, corresponding to center of mass energy of $\approx$ 300 GeV. In 1998 HERA switched to electrons of 27.5 GeV, now colliding on protons with increased beam energy of 920 GeV, corresponding to an increased $\sqrt{s}$ of $\approx$ 320 GeV.

1.2. Cross Sections

In neutral current (NC) the interaction is mediated by a γ or Z boson. The double differential inclusive cross section is given by:

$$\frac{d^2\sigma^{e^\pm p\to e^\pm X}}{dx\,dQ^2} = \frac{2\pi\alpha^2}{xQ^4}[Y_+\tilde{F}_2(x,Q^2) - y^2F_{_L}(x,Q^2) \mp Y_- xF_3(x,Q^2)] \quad (1)$$

α is the fine structure constant, $Y_\pm = 1 \pm (1-y)^2$.

The dominant contribution to the cross section is the generalized proton structure function $\tilde{F}_2$, with contribution from the purely electromagnetic proton structure function F_2^{em} and contributions from γZ interference and pure Z exchange, the latter two are suppressed by propagator terms. The contribution of the longitudinal structure function $F_{_L}$ to the presented cross sections is $< 5\%$ at the highest y values and is negligible for $y < 0.4$. The parity violating structure function xF_3 contributes with different sign to electron and positron cross sections.

The NC cross section measurement is presented in the form of the reduced cross section defined as:

$$\tilde{\sigma}_{NC}(x,Q^2) = \frac{xQ^4}{2\pi\alpha^2}\frac{1}{Y_+}\frac{d^2\sigma_{NC}}{dx\,dQ^2} \quad (2)$$

At low Q^2 and small y, where xF_3 and $y^2F_{_L}$ can be neglected, the reduced cross section coincides with F_2.

In the charged current (CC) case the interaction is mediated by a charged boson, $W^\pm$, and the cross section is given by:

$$\frac{d^2\sigma_{CC}}{dx\,dQ^2} = \frac{G_F^2}{2\pi x}\left(\frac{{M_W}^2}{{M_W}^2+Q^2}\right)^2\Phi_{CC}(x,Q^2) \quad (3)$$

$$\Phi_{CC}^{e^+p}|_{LO} = x\left((\bar{u}+\bar{c}) + (1-y)^2(d+s)\right) \quad (4)$$

$$\Phi_{CC}^{e^-p}|_{LO} = x\left((u+c) + (1-y)^2(\bar{d}+\bar{s})\right) \quad (5)$$

with the Fermi coupling constant G_F and the mass of the W boson M_W. The CC measurement

is presented in the form of the helicity weighted parton densities Φ_{CC}.

2. EXPERIMENTAL TECHNIQUES

2.1. H1 Detector

The H1 detector is described elsewhere in detail [1]. The most important device for the NC and CC analyses is the Liquid Argon (LAr) Calorimeter [2]. It is constructed as a sampling calorimeter with a high granularity of 45000 cells. The calorimeter has an angular acceptance of $4^\circ < \theta < 156^\circ$ where θ is the polar angle of the scattered lepton with respect to the proton beam direction. After calibration the uncertainty on the electromagnetic energy scale is 1%-2% in the backward region ($\theta_e > 90^\circ$) and 3% in the forward region. The hadronic energy scale has an uncertainty of 3% (4%) in the forward (backward) part.

The central and forward tracking chambers are used to measure the vertex, to support electron identification, and to improve the measurement of the polar and azimuthal angles of the scattered electron (positron).

2.2. Kinematic Reconstruction

The measurement of the differential DIS cross sections relies on the precise determination of the kinematic variables associated with the interaction. For the CC inclusive scattering process $ep \to \nu X$, these variables can only be reconstructed using the hadronic final state. For the NC case, the reconstruction of the scattered electron (positron) and of the hadronic final state properties allows several complementary approaches to the kinematic reconstruction [3–6].

2.3. Event Selection

The presented analyses for positron proton collisions are based on the e^+p luminosity of 36 pb^{-1} accumulated in 1994-97. Preliminary results of the electron proton analyses were derived from 5.3 pb^{-1} of the ongoing e^-p data taking.

The selection of high Q^2 neutral current events is based on the identification of the scattered electron. It is selected by requiring a compact electromagnetic energy deposit in the LAr calorimeter with an energy $E' > 11$ GeV, linked to a track. Further selection criteria are applied to suppress photoproduction background and to reduce radiative corrections.

The main selection criteria for charged current events is an imbalanced transverse momentum, $P_t > 12$ GeV, measured in the LAr calorimeter as the outgoing (anti)neutrino escapes detection. Photoproduction background is rejected by requiring that the transverse energy flow is predominantly oriented into one hemisphere. The measurement is limited to the range $0.03 < y < 0.9$. Cosmic ray and beam halo backgrounds are suppressed by a set of topological background filters. The data sample is cleaned from non ep events by a visual scan.

3. RESULTS

3.1. e^+p NC and CC results

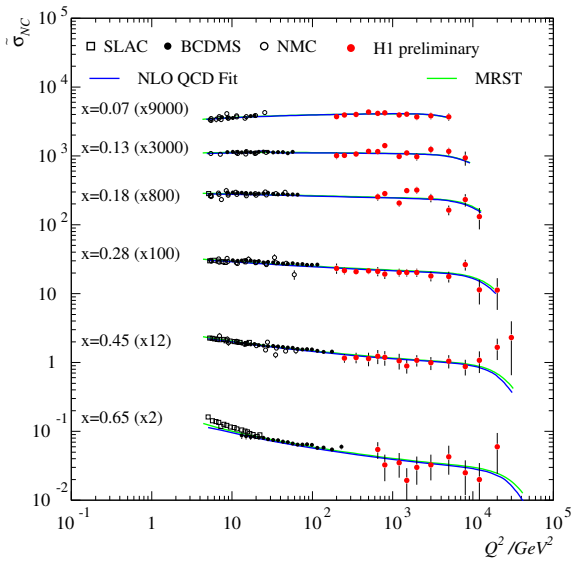

Figure 1. The reduced neutral current cross section at high x compared with the Standard Model expectations

The preliminary reduced neutral current cross section measurement by H1 is shown in Fig. 1

together measurements from fixed target experiments as function of Q^2 at fixed values of x, $x \leq 0.07$. The cross section is compared to the SM expectation from a QCD evolution with given input parton densities [7]. At $x = 0.45$ an excess of the cross section over the SM prediction is visible for the highest Q^2 values. For $x < 0.45$ $\tilde{\sigma}_{NC}$ starts to drop at Q^2 values of about 8000 GeV^2, the mass of the Z squared, due to the destructive γZ interference.

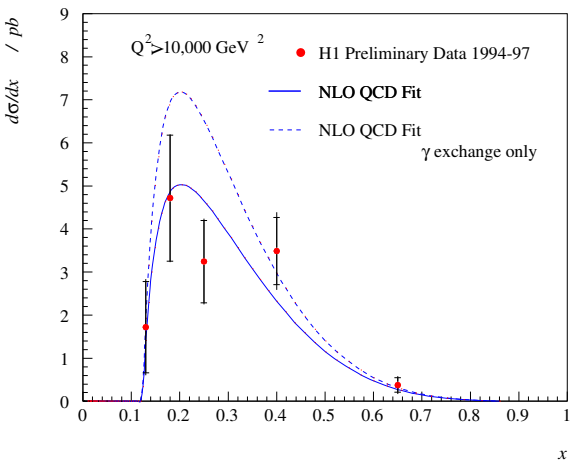

Figure 2. Single differential cross section $d\sigma/dx$ at $Q^2 > 10000$ GeV^2 compared with the SM expectation and a model where contributions from Z exchange are omitted.

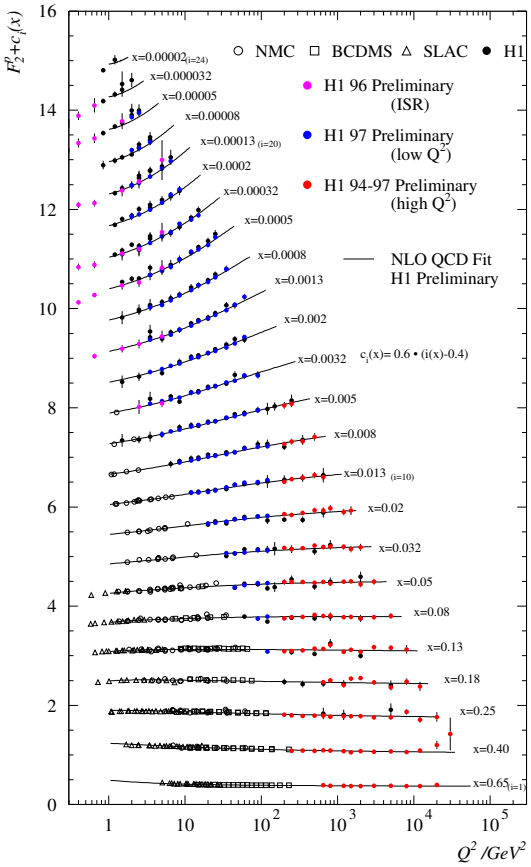

Figure 3. $F_2^p (\equiv F_2^{em})$ results for $Q^2 \approx$ 1 to 30000 GeV^2, and x between .00002 and 0.65.

Sensitivity to the γZ interference in e^+p interaction is shown in Fig. 2, where the single differential cross section $d\sigma/dx$ at $Q^2 > 10000$ GeV^2 is compared with the SM expectation and a model where the Z contributions have been omitted artificially. The predictions are significantly different and the data are in favour of the SM prediction where the e^+p cross section is suppressed.

Taking into account contributions from F_L and Z exchange, the proton structure function $F_2^p (\equiv F_2^{em})$ can be extracted from the double differential NC cross section. Fig. 3 shows the preliminary measurements combined with H1 low Q^2 data where the positron is detected in the backward electromagnetic calorimeter Spacal and with data from fixed target experiments.

The double differential CC cross section as function of x for $400 \leq Q^2 \leq 16000$ GeV^2 is compared to Standard Model expectation in Fig. 4. At low x the cross section is dominated by the antiquark density $(\bar{u} + \bar{c})$, while at $x > 0.2$ the cross section is almost entirely determined by the d quark.

From the Q^2 dependence of the CC cross section the W mass M_W has been extracted from

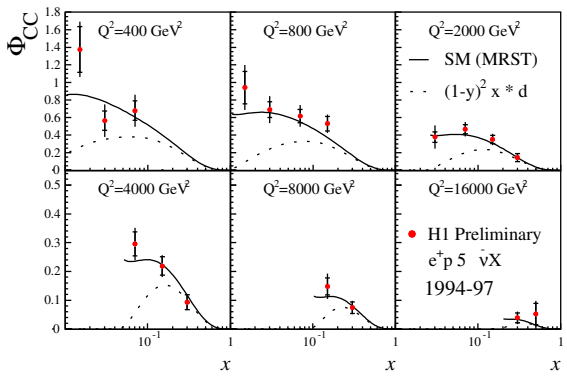

Figure 4. Double differential e^+p CC cross section as function of x at fixed values of Q^2 compared with the Standard Model expectation. The expected contribution of the d quark is given by the dashed line.

e^+p- CC processes, yielding

$$M_W = 81.2 \pm 3.3(\text{stat.}) \pm 4.3(\text{sys.}) \text{ GeV} \qquad (6)$$

which is in agreement with the world average.

3.2. First Results from 1998/99 e^- running

The single differential NC and CC cross sections $d\sigma/dQ^2$ for e^-p interactions are shown in Fig. 5 compared to cross section measurements from e^+p collisions.

The measurements of NC cross sections span more than two orders of magnitude in Q^2. The rapid fall with Q^2 by about 6 orders of magnitude is well reproduced by the SM predictions. In agreement with SM prediction for γZ interference the e^-p cross section is above e^+p for $Q^2 \geq 3000$ GeV^2. The increase of the center of mass energy in e^-p collisions does not influence this conclusion.

At low Q^2 the CC cross sections are suppressed by the propagator. With increasing Q^2 CC cross sections are approaching the NC cross sections. The e^-p CC cross section exceeds that of e^+p by almost a factor of 10 at large Q^2 due to the coupling to different flavours (u and d, respectively) and the helicity factor (equations 4 and 5).

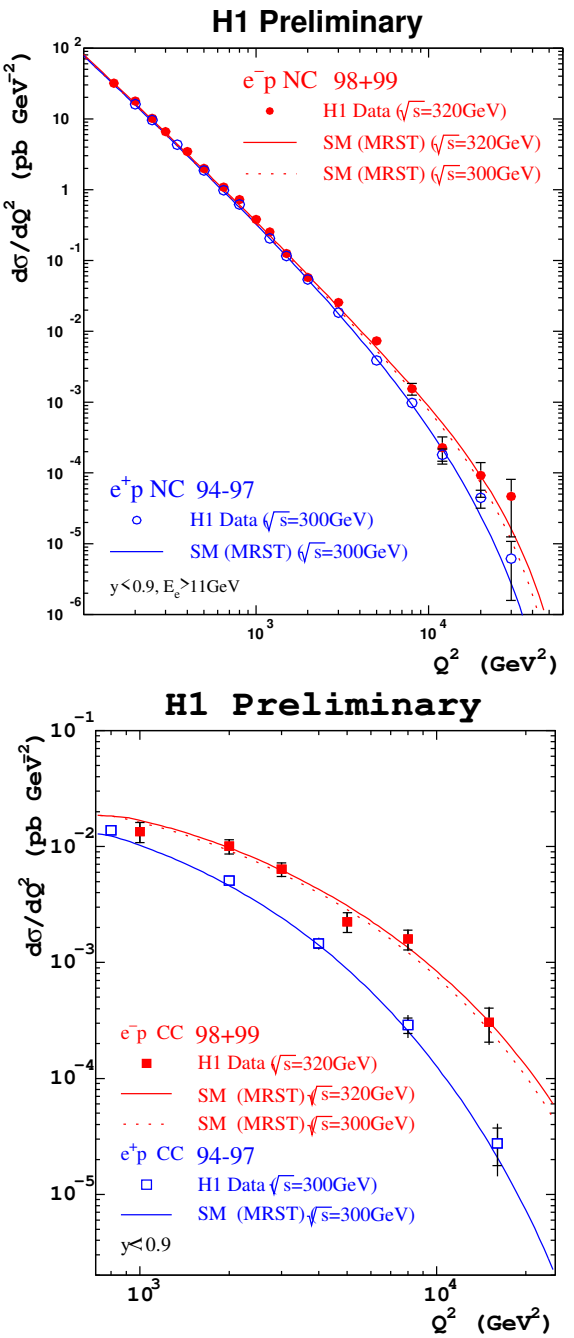

Figure 5. Single differential NC and CC cross section $d\sigma/dQ^2$ for e^-p and e^+p interactions compared with the Standard Model expectations.

4. SUMMARY

Neutral and charged current processes have been studied at H1. Double differential e^+p and single differential $e^\pm p$ cross sections have been measured up to $Q^2 = 30000$ GeV^2. The SM is in agreement with the measurements, except for the region of high $Q^2 > 15000$ GeV^2 where an excess of the NC e^+p data is seen at the level of about 2 standard deviations.

In the comparison of e^-p and e^+p NC cross sections the positive (negative) contribution of γZ interference is observed.

The CC cross section measurements constrain the valence d and u quark distributions. The Q^2 dependence of the CC cross section has been exploited to determine the W mass. The predictions for the electroweak sector of the Standard Model are in agreement with the measurements.

Acknowledgments: I would like to thank my colleagues in H1 for providing a wealth of information. We are grateful to the HERA machine group whose outstanding efforts have made and continue to make this experiment possible.

REFERENCES

1. H1 Collab., I.Abt et al., Nucl. Instr. Meth. **A386** (1997) 310 and 348.
2. H1 Calorimeter Group, B.Andrieu et al., Nucl. Instr. Meth. **A336** (1993) 460.
3. A.Blondel, F.Jacquet, Proceedings of the Study of an *ep* Facility for Europe, ed. U.Amaldi, DESY 79/48 (1979) 391.
4. U.Bassler and G.Bernardi, Nucl. Instr. Meth. **A361** (1995) 197.
5. U.Bassler and G.Bernardi, Nucl. Instr. Meth. **A426** (1998) 583.
6. S.Bentvelsen et al., Proceedings of the Workshop Physics at HERA, vol. 1, eds. W.Buchmüller,G.Ingelman, DESY (1992) 23. C.Hoeger,ibid.,43.
7. A.Martin el al., RAL-TR-98-029.